J. Fluid Mech. (1984), *vol.* 139, *pp.* 193–218
Printed in Great Britain

A turbulent-transport model for concentration fluctuations and fluxes

By R. I. SYKES, W. S. LEWELLEN AND S. F. PARKER
Aeronautical Research Associates of Princeton, Inc., 50 Washington Road, P.O. Box 2229, Princeton, New Jersey 08540

(Received 31 March 1983)

A second-order closure model describing the diffusion of a passive scalar from a small source is presented. The model improves upon the earlier work of Lewellen & Teske (1976) by ensuring the early stage of the release, the so-called meander phase, is accurately described. In addition to the mean concentration and scalar fluxes, a model equation for the evolution of the scalar variance is proposed. The latter introduces a new lengthscale which represents the scale of the concentration fluctuations. The model predictions are compared with the recent experimental data of Fackrell & Robins (1982*a*, *b*).

1. Introduction

The problem of predicting the dispersal of a pollutant in a turbulent flow is of enormous importance, and has received considerable attention from researchers. Although there is an extensive literature on the subject, practical prediction methods have not progressed much beyond the Gaussian plume formulae or the eddy-diffusivity models. There is, however, a broad basis of more fundamental research on turbulent diffusion of a scalar field, both experimental and theoretical, which can be used to provide the necessary insight to develop an improved prediction method. Most of the more fundamental theoretical methods present very severe problems in their extension to non-homogeneous or time-dependent turbulent fields, so that some intermediate level is required. The second-order closure framework provides such a level, in that more of the physical processes are contained within the equations than with eddy-diffusivity models, but the equations are still considerably simpler than a spectral closure (see e.g. Leslie 1973).

A further advantage of closure at second order is the inclusion of fluctuating scalar concentration variance, since this is a second-order correlation. Given the scalar variance, and an integral timescale for the concentration fluctuations, it is possible to estimate the uncertainty in likely measured values for different averaging times. This natural variability, which should be considered for proper evaluation of atmospheric dispersion models, may be important for sampling times as long as one hour under some conditions. Knowledge of the higher-order moments of the probability density function for the scalar field can be particularly valuable in situations where instantaneous or very short time averages are important, for example in the dispersion of toxic or flammable gases, or in assessing the problem of detectable odours. In these cases, the ensemble-mean concentration may be well below the threshold value, but the locally measured value can still exceed the limit for short times and cause problems.

The application of second-order closure models to the diffusion of a scalar has

received less attention than that of the transport of momentum and heat (e.g. Lewellen 1977; Launder, Reece & Rodi, 1975; Lumley & Khajeh-Nouri 1974). The development of such a model for dispersion in the atmosphere was first given by Donaldson (1973). Lewellen & Teske (1976) presented the results of a simple second-order closure model for dispersion in the atmospheric boundary layer. Their model was able to describe the two stages of diffusion from a small source, namely the initial or meander plume where the plume dimensions grow linearly and the late phase where the plume spreads with a constant diffusivity; this behaviour is consistent with Taylor's (1921) diffusion theory. Lewellen & Teske (LT) showed how the transition between the two stages was accomplished in the model by a change in balance in the scalar flux equation. Deardorff (1978) elucidated the model dynamics by presenting an exact solution for an exponential autocorrelation in homogeneous turbulence and showing that the second-order closure model could reproduce the result. The study of El Tahry, Gosman & Launder (1981) also demonstrates the ability of second-order closure to describe scalar dispersion, but is limited in its application, since it uses an algebraic model for the fluxes, which cannot describe the early evolution from a small source.

The objective of this paper is to improve the LT second-order closure model for the mean concentration and to develop a model for the concentration variance in a non-homogeneous flow. We shall use analytical and experimental results in designing the modelled terms wherever possible, and our principal comparison with laboratory data will be the recent experiment by Fackrell & Robins (1982*a*), who measured turbulent correlations in a plume diffusing in a wind-tunnel boundary layer. We shall first discuss diffusion in homogeneous turbulence to help clarify the basic timescales of the problem. Recent experimental work by Warhaft & Lumley (1978) on the decay of homogeneous scalar variance, has shown that the scalar field introduces its own lengthscale into the dynamics. The presence of more than one timescale is also emphasized in the theoretical descriptions using spectral closure (Newman & Herring 1979), large-eddy simulation (Antonopoulos-Domis 1981), second-order closure (Newman, Launder & Lumley 1981) and random-walk simulation (Durbin 1982). Having determined the appropriate timescales and turbulence model, we shall then proceed to the non-homogeneous boundary-layer studies by Fackrell & Robins (1982*a*).

2. Diffusion in homogeneous turbulence

2.1. *Mean concentration*

We consider the diffusion of a passive scalar in a homogeneous turbulent field in the limit of large Péclet and Reynolds numbers. Let $c(\boldsymbol{x}, t)$ denote the scalar field, and let the overbar represent an ensemble average. Then

$$\frac{\mathrm{D}\bar{c}}{\mathrm{D}t} = -\frac{\partial}{\partial x_i}\overline{u_i' c'}, \tag{2.1}$$

where

$$\frac{\mathrm{D}}{\mathrm{D}t} \equiv \frac{\partial}{\partial t} + \bar{u}_j \frac{\partial}{\partial x_j},$$

and a prime denotes a fluctuating quantity, e.g. $c' = c - \bar{c}$; u_i is the velocity component in the coordinate direction x_i.

The equation for the turbulent concentration flux is

$$\frac{\mathrm{D}}{\mathrm{D}t}\overline{u_i'c'} = -\overline{u_i'u_j'}\frac{\partial \bar{c}}{\partial x_j} - \overline{u_j'c'}\frac{\partial \bar{u}_i}{\partial x_j} - \frac{\partial}{\partial x_j}\overline{u_i'u_j'c'} - \frac{1}{\bar{\rho}}\overline{c'\frac{\partial p'}{\partial x_i}}, \tag{2.2}$$

where p' is the pressure fluctuation and $\bar{\rho}$ the mean density. We have assumed that the molecular dissipation term is isotropic, and therefore vanishes in (2.2).

In this section we consider the source term to consist of an instantaneous line release of zero dimension, so that at $t = 0$

$$\bar{c}(y, z, t = 0) = Q\delta(y)\,\delta(z),$$

where δ is the Dirac delta function, Q is the mass released per unit length in the x_1 direction, and we have identified y and z with the x_2 and x_3 coordinates respectively.

Deardorff (1978) shows that the exact solution should be expected to be Gaussian with a spread in the y-direction given by

$$\sigma_y^2 = 2\overline{v'^2}\tau^2\left\{\frac{t}{\tau} - 1 + \exp\left(\frac{-t}{\tau}\right)\right\}, \tag{2.3}$$

where $\sigma_y^2 = (1/Q)\int\int y^2\bar{c}(y, z, t)\,\mathrm{d}y\,\mathrm{d}z$. A similar equation holds for σ_z^2, with $\overline{w'^2}$ replacing $\overline{v'^2}$ in (2.3). The timescale τ in (2.3) is the integral timescale of the Lagrangian velocity autocorrelation function, which was assumed to be exponential. In fact, Deardorff only considered the one-dimensional diffusion problem, but it is easily extended to two dimensions with the assumption that $\overline{v'w'} \equiv 0$. The latter can always be assured by a rotation of the (y,z)-coordinate axes.

We first note that the triple-moment term does not affect the calculation of σ_y^2 or σ_z^2, as shown by Lewellen (1981), provided that the triple is modelled as a gradient term. Thus the only modelled term affecting the development of the plume lengthscales is the pressure correlation. Deardorff shows that this term needs to be modelled as

$$\frac{1}{\bar{\rho}}\overline{c'\frac{\partial p'}{\partial x_i}} = \frac{\overline{u_i'c'}}{\tau}.$$

In accordance with earlier work (Lewellen 1977), we model this term as $A(q/\Lambda)\,\overline{u'c'}$, where $q^2 = \overline{u_i'u_i'}$, and Λ is a turbulent lengthscale defined so that the dissipation of turbulent kinetic energy is $q^2/8\Lambda$. A is a numerical constant, which takes a value of 0.75. Note that this model is closer to that originally proposed by Donaldson (1973) than to the LT model, which used a timescale corresponding to the turbulent timescale in the region of the spectrum defined by the plume scale. The longer timescale Λ/Aq now seems more appropriate in the light of Deardorff's result. We can interpret this physically as saying that, even when the plume is very small, the diffusion is effected by large-scale meandering of the plume, so that the flux is carried by the ambient energy-containing eddies on the lengthscale Λ, having a timescale of order Λ/q. The latter ambient turbulent timescale is therefore the appropriate timescale for the pressure correlation term in the scalar flux equation, although other terms in the equations will depend on plume turbulent timescales.

The triple moment in (2.2) determines the shape of the mean-concentration profile in the early stages of the dispersion. Deardorff shows that the triple-moment term can be modelled as

$$\frac{\partial}{\partial x_j}\overline{u_i'u_j'c'} = \frac{\partial}{\partial x_j}\left(K_{jm}\frac{\partial}{\partial x_m}\overline{u_i'c'}\right), \tag{2.4}$$

where K_{jm} has to take a certain time-dependent form to ensure a Gaussian profile. In fact, the requirement can be stated more clearly when one notes that the Gaussian profile is a self-similar profile, so that all moments and correlations are diffusing at the same rate and thus preserve the shape. This means that, when we close the equations and model a diffusive term empirically, we must ensure that all the correlations are diffusing at the same rate to obtain a self-similar solution. For closure at second order, (2.4) is thus the appropriate closure with K_{jm} obtained from the diffusion of the mean concentration. In order to keep the model as simple as possible, bearing in mind our desire to extend it to more complex flows, we choose to estimate K_{jm} as

$$K_{jm} = \frac{1}{Q}\int\int (x_j \overline{u'_m c'} + x_m \overline{u'_j c'})\,\mathrm{d}y\,\mathrm{d}z. \tag{2.5}$$

This will correspond exactly to Deardorff's value in the case of homogeneous turbulence at short time, and will provide a robust estimate for more complex situations. Using this closure model, it follows from Deardorff's analysis that the equations do predict a Gaussian mean profile with the correct spread rate. This model is also different from LT, so that the latter does not predict Gaussian profiles.

At late times, LT show that the balance in equation (2.2) is between production and pressure scrambling, i.e.

$$-\overline{u'_i u'_j}\frac{\partial \bar{c}}{\partial x_j} - \frac{Aq}{\Lambda}\overline{u'_i c'} = 0,$$

so that we have gradient diffusion with an effective viscosity $K_{jm} = \overline{u'_j u'_m}\,\Lambda/Aq$. In this late-time limit the diffusivities calculated from (2.5) will yield this same value.

Our model for the mean concentration and its fluxes is therefore

$$\frac{\mathrm{D}\bar{c}}{\mathrm{D}t} = -\frac{\partial}{\partial x_i}\overline{u'_i c'},$$

$$\frac{\mathrm{D}}{\mathrm{D}t}\overline{u'_i c'} = -\overline{u'_i u'_j}\frac{\partial \bar{c}}{\partial x_j} - \overline{u'_j c'}\frac{\partial \bar{u}_i}{\partial x_j} + \frac{\partial}{\partial x_j}\left(K_{jm}\frac{\partial}{\partial x_m}\overline{u'_i c'}\right) - \frac{Aq}{\Lambda}\overline{u'_i c'}, \tag{2.6}$$

where

$$K_{jm} = \frac{\langle x_j \overline{u'_m c'} + x_m \overline{u'_j c'}\rangle}{\langle \bar{c}\rangle}$$

and $\langle\phi\rangle = \int\int \phi\,\mathrm{d}y\,\mathrm{d}z$.

Deardorff criticizes the LT model on the grounds that K_{jm} is a function of time since release. We have removed the explicit dependence on time in K_{jm}, and replaced it with a value that depends on the local state of the plume; this permits individual plumes to be treated separately. Thus the second-order closure model possesses several advantages over first-order closure. First, the diffusion process is described in terms of the more fundamental turbulence quantities rather than an empirical eddy diffusivity. Note that we have avoided the necessity to specify such an eddy diffusivity for the second-order quantities by using (2.5), which is the effective diffusivity predicted by the closure model itself. Secondly, the second-order closure provides a definite framework for extending the model to non-homogeneous or buoyancy-driven flows. Finally, a prediction of scalar variance is a natural part of the second-order closure model, so that we obtain significantly more information about the concentration distribution. As we shall demonstrate, modelling the scalar variance introduces a new lengthscale which represents the scale of the concentration fluctuations; this scale grows as the plume grows, so that the time since release is dynamically significant.

2.2. *Concentration-fluctuation variance*

There have been a number of studies, both theoretical and experimental, of the variance of concentration fluctuations. Gifford (1959) proposed a relatively simple phenomenological model for the early or meander stage of a plume in terms of two plume lengthscales but did not prescribe a method for predicting the scales themselves. Chatwin & Sullivan (1979*a*, *b*, 1980) investigated theoretically the relative diffusion of a cloud of marked particles and demonstrated that the variance depends on source size, so that it is meaningless to consider a point source. They did not include molecular dissipative effects rigorously, however, and comparison with any second-order closure result is further precluded by their examination of the relative diffusion as opposed to the ensemble average. Unfortunately, the latter is also true of their measured data, and also the data of Murthy & Csanady (1971).

Durbin (1980) used a two-particle random walk model to predict the concentration variance. His model includes the effect of small molecular diffusivity by averaging the fluctuations over a small volume. Functional forms for the one- and two-particle time and space correlations are chosen to be consistent with an inertial range at small separation, and exponential in time. Several predictions are made by homogeneous turbulence, but there is no quantitative comparison with data.

There have been a number of studies of the decay of homogeneous scalar variance, as mentioned in the introduction, but we shall concentrate on the diffusion from a small source since our main interest lies in this direction.

Fackrell & Robins (1982*b*) have recently completed Gifford's fluctuating plume model and used it to predict concentration variance $\overline{c'^2}$, which is compared with laboratory data for an elevated source in a wind-tunnel boundary layer. Gifford's model requires prediction of the outer scale of the plume, i.e. the scale over which the plume meanders, and the inner or instantaneous plume scale, i.e. the relative spread of the plume. Fackrell & Robins used the statistical formulations of Hay & Pasquill (1959) and Smith & Hay (1961) to predict these scales in terms of the measured Eulerian velocity spectra. The Smith–Hay model has been criticized by Sawford (1982) for slow growth during part of the range for a very small source, but the formulation is consistent with other approximations over most of the range. Fackrell & Robins demonstrate reasonable agreement with the observations using this simple model, indicating that the model probably contains the correct basic physics. We wish to include these processes within a second-order closure framework, and we shall therefore draw on this model to assist in the determination of closure assumptions.

The Reynolds-averaged equations for the concentration variance is

$$\frac{\mathrm{D}}{\mathrm{D}t}\overline{c'^2} = -2\overline{u_i' c'}\frac{\partial \bar{c}}{\partial x_i} - \frac{\partial}{\partial x_i}\overline{u_i' c'^2} - \epsilon_c, \tag{2.7}$$

where ϵ_c represents the dissipation of $\overline{c'^2}$ by molecular diffusion. Since $\overline{c'^2}$ should diffuse with the turbulent correlations, we model the triple-correlation term as in the flux equations. Thus we set

$$-\frac{\partial}{\partial x_i}\overline{u_i' c'^2} = \frac{\partial}{\partial x_j}\left(K_{ij}\frac{\partial}{\partial x_i}\overline{c'^2}\right),$$

where K_{ij} is given by (2.5).

In earlier work (LT, Lewellen 1977), ϵ_c has been modelled as $0.45\,\overline{c'^2}/\tau_c$, where τ_c is a dissipation timescale, calculated from the turbulence timescale in the region of the ambient turbulent spectrum defined by the plume scales σ_y and σ_z. This formulation is not correct, because σ_y and σ_z are the outer or meander scales, which

Fackrell & Robins show become rapidly independent of the source, while the total $\overline{c'^2}$ is largely a result of the disparity between the inner and outer scales, and the inner scale remembers its initial condition for much longer. We therefore require an inner scale, Λ_c, which we shall then use to determine τ_c.

The basis of the Smith–Hay model for the inner scale is a selective filter on the velocity spectrum, which states in effect that the inner scale will grow at a rate proportional to the scale of the velocity fluctuations in the part of the spectrum corresponding to the inner scale itself. We can derive a much simpler equation for Λ_c by assuming that the turbulent energy decays in a manner consistent with an inertial range for scales much less than the turbulent lengthscale Λ. In practical situations, some such assumption will be necessary, since turbulent spectra will not generally be available. We therefore set

$$q_c = q\left(\frac{\Lambda_c}{\Lambda}\right)^{\frac{1}{3}} \quad (\Lambda_c \ll \Lambda) \tag{2.8}$$

and

$$\frac{\mathrm{d}\Lambda_c}{\mathrm{d}t} = \alpha_1 q_c, \tag{2.9}$$

where α_1 is an $O(1)$ constant, to be determined from comparison with data. Note that (2.8) and (2.9) give the expected initially linear growth with t, followed by a region with $\Lambda_c \propto t^{\frac{3}{2}}$ (see e.g. Sawford 1982). The dissipation timescale τ_c is then constructed from q_c and Λ_c, so that our model for ϵ_c is

$$\epsilon_c = \alpha_2 \frac{q_c}{\Lambda_c} \overline{c'^2}, \tag{2.10}$$

where α_2 is a second constant.

Note that our dissipation model depends entirely upon inertial properties of the velocity field, i.e. explicit molecular-diffusivity effects are absent. This means that our model is only applicable for high-Péclet-number flows, i.e. flows in which $\Lambda_c \gg \eta_c$, where η_c is the dissipation scale $\kappa_c^{\frac{3}{4}} \epsilon^{-\frac{1}{4}}$; κ_c is the molecular diffusivity of the scalar, and ϵ is the turbulent energy dissipation rate. Λ_c must also be much larger than the Kolmogorov scale $\nu^{\frac{3}{4}} \epsilon^{-\frac{1}{4}}$, where ν is the kinematic viscosity. In the experiment of Fackrell & Robins (1981), the dissipation scales are roughly 0.1 mm, while the smallest source diameter is 3 mm.

An analytic solution for the early-time behaviour is obtained in Appendix A, and we summarize the results here. We denote by δ the source-scale to turbulence-scale ratio, i.e. $\sigma_0/\Lambda = \delta$, and define Λ/q as the unit time. Then, the production of $\overline{c'^2}$ is important only for $t < O(\delta)$; the maximum value of $\hat{c}/C_\mathrm{m}$ is $O(\delta^{-\frac{1}{3}})$, and occurs at $t = O(\delta^{\frac{2}{3}})$. Here $\hat{c}^2$ and C_m are the maximum values of fluctuation variance and mean concentration respectively in the plane transverse to the mean flow. These results are in good agreement with the data of Fackrell & Robins for their elevated release; they suggest that $\overline{c'^2}$ is a maximum at $t = O(\delta)$, while the maximum $\hat{c}/C_\mathrm{m}$ is $O(\delta^{-0.4})$ at $t = O(\delta^{0.7})$. Thus our model for the dissipation of $\overline{c'^2}$ contains the correct timescales, and we shall fix α_1 and α_2 to optimize quantitative agreement with the laboratory data of Fackrell & Robins. We emphasize that in this section we are treating the elevated releases as homogeneous turbulence; this is a good approximation for the early part of the release, and we shall show in §3 that a more complete treatment of the effect of the wall does not significantly alter the predictions of $\hat{c}/C_\mathrm{m}$.

Before attempting to fix α_1 and α_2, we should recognize that eventually Λ_c will grow

to be as large as Λ, so that (2.8)–(2.10) will be inappropriate. Λ_c will continue to grow, since different parts of the plume will continue to separate. Λ_c is related to Durbin's (1980) particle separation Δ, which grows like $t^{\frac{1}{2}}$ at late times, so a simple model which gives the correct asymptotic behaviour is

$$\frac{\mathrm{d}\Lambda_c}{\mathrm{d}t} = \beta_1 q \frac{\Lambda}{\Lambda_c} \quad (\Lambda_c \gg \Lambda). \tag{2.11}$$

Our philosophy here is to establish various asymptotic limits for modelled terms, and then match smoothly with the simplest type of function. In view of the complexity introduced by the presence of multiple scales, some firm idea of the behaviour in different limits is vital to the development of a physically realistic model. We now need to determine the dissipation timescale for $\overline{c'^2}$ when $\Lambda_c \gg \Lambda$. The timescale in (2.10) for $\Lambda_c \ll \Lambda$ can be derived by an inertial-range argument on the basis of Péclet-number independence, so that the spectral transfer of $\overline{c^2}$ towards large wavenumber depends only on the local values in wavenumber space. A similar argument for $\Lambda_c \gg \Lambda$ would require the knowledge of energy-spectrum decay at small wavenumbers, but it appears that local wavenumber interactions are not the principal mechanism for transfer down the spectrum when $\Lambda_c \gg \Lambda$. Rigorous analysis is, of course, virtually impossible at present, but the Test Field Model of Newman & Herring (1979) is a spectral closure giving some insight into the dynamics. The TFM predicts that in the limit $\Lambda_c \gg \Lambda$ the dominant interactions removing $\overline{c'^2}$ stuff from the Λ_c scale involve the energy-containing eddies on the scale Λ. Thus the timescale for the decay of $\overline{c'^2}$ as obtained from the TFM is $O(\Lambda_c/q)$, i.e. the large scale of the concentration fluctuations with the full turbulence energy. We therefore model the dissipation as

$$\epsilon_c = \beta_2 \frac{q}{\Lambda_c} \quad (\Lambda_c \gg \Lambda). \tag{2.12}$$

At this stage we have fixed asymptotic behaviour at both extremes of Λ_c, and introduced four empirical constants. This is somewhat misleading because Λ_c has not been defined precisely except in terms of the dissipation ϵ_c, so that there are actually only two constants. To make this clearer, and also to fix one of the constants, we consider the dispersion of a plume from a point source in decaying homogeneous turbulence. Gad-el-Hak & Morton (1979) performed such an experiment and obtained a self-similar profile of $(\overline{c'^2})^{\frac{1}{2}}/\bar{c}$ across the plume well downstream of the source. We are unable to model the initial development of the plume, since the scalar was introduced in a jet which causes the initial phase to be non-homogeneous turbulence. However, it is claimed that the jet decays very quickly and we can consider their measured profiles to represent the late stages of dispersion in homogeneous turbulence.

The second-order closure model predicts power-law decay of the turbulence energy (Lewellen 1977) and growth of the lengthscale Λ with exponents $-\frac{5}{4}$ and $\frac{3}{8}$ respectively. If we substitute these quantities into the plume equations, it is possible to obtain a self-similar form for $\overline{c'^2}$. We note that the mean concentration will spread as a Gaussian at the same rate as Λ, with the fluxes proportional to the mean-concentration gradient. The mean concentration has the similarity form

$$\bar{c}(r,t) = \frac{Q_0}{\sigma^2} \exp\left(-\frac{r^2}{\sigma^2}\right), \tag{2.13}$$

where r is the radial distance from the centre of the plume, Q_0 is a constant

proportional to the mass flux in the plume, and σ is the spread of the plume, so that $\sigma \propto t^{\frac{3}{8}}$. If we postulate a similarity form for $\overline{c'^2}$, namely

$$\overline{c'^2}(r,t) = \frac{Q_0^2}{\sigma^4} f(\xi), \tag{2.14}$$

where $\xi = r/\sigma$, we can obtain an equation for f as

$$f'' + \left(\xi + \frac{1}{\xi}\right) f' + (4 - \Gamma) f = -2\xi^2 \mathrm{e}^{-2\xi^2}, \tag{2.15}$$

where Γ is a constant which depends on the Λ_c equation. If we use the large-Λ_c equations for Λ_c and ϵ_c, then

$$\Gamma = \beta_2 \left(\frac{40}{3\beta_1}\right)^{\frac{1}{2}}; \tag{2.16}$$

this choice will be justified *a posteriori*. This similarity equation has precisely the same form as that proposed by Csanady (1967), except that Csanady chose his form for ϵ_c so that he obtained the similarity equation for non-decaying turbulence. Our specification predicts no similarity for that case, but the experimental details furnished by Csanady are not sufficient to determine whether there is any real inconsistency with observations. However, the data of Gad-el-Hak & Morton do suggest similarity, and we choose the constant Γ to fit their data. Figure 1 shows the predicted form for $(\overline{c'^2})^{\frac{1}{2}}/\bar{c}$ using $\Gamma = 4.6$ and $\Gamma = 5.2$ together with the data of Gad-el-Hak & Morton. We choose to use $\Gamma = 4.6$, implying $\beta_2/\beta_1^{\frac{1}{2}} = 1.26$; this provides a reasonably good fit for the range of the data with largest errors at the origin.

As we noted earlier, this large-Λ_c formulation only involves one constant, namely $\beta_2/\beta_1^{\frac{1}{2}}$, which we have now fixed at 1.26. The small-Λ_c formulation similarly involves only one constant. There remains the problem of joining the two asymptotic regimes, and we accomplish this by making the simple postulate that the two regimes match at a certain point, say $\Lambda_c = c_0 \Lambda$. Then, from (2.8)–(2.12),

$$\beta_1 = \alpha_1 c_0^{\frac{4}{3}} \tag{2.17}$$

and

$$\beta_2 = \alpha_2 c_0^{\frac{2}{3}}, \tag{2.18}$$

so that we have three relations between the five constants α_1, α_2, β_1, β_2 and c_0 in total. There is still an arbitrary factor in the definition of Λ_c, but this is removed by setting the initial value of Λ_c equal to the initial σ_y of the plume. There are thus two more constants with which to optimize model performance; we fix α_1 and α_2, then the above relations will determine c_0, β_1, β_2.

The elevated release data of Fackrell & Robins (1982*a*) provides the evolution of $\overline{c'^2}$ and $\bar{c}$ for a range of source sizes. The latter part of the measurements are affected by the presence of the wall, but the first half is near-homogeneous flow conditions. In order to fix α_1 and α_2, we set the background turbulence values to the observed values at the source height, and solve the parabolic problem marching in the streamwise direction with the observed mean speed. The plume was initialized as a Gaussian shape $\sigma_y = \sigma_z = \frac{1}{2}d_s$, where d_s is the diameter of the source, and $\overline{c'^2}$ was set to zero initially. Λ_c is also set at $\frac{1}{2}d_s$ initially, and the background turbulence scale Λ is obtained from the empirical formula

$$\frac{1}{\Lambda} = \frac{1}{0.65 z_s} + \frac{1}{0.2H}, \tag{2.19}$$

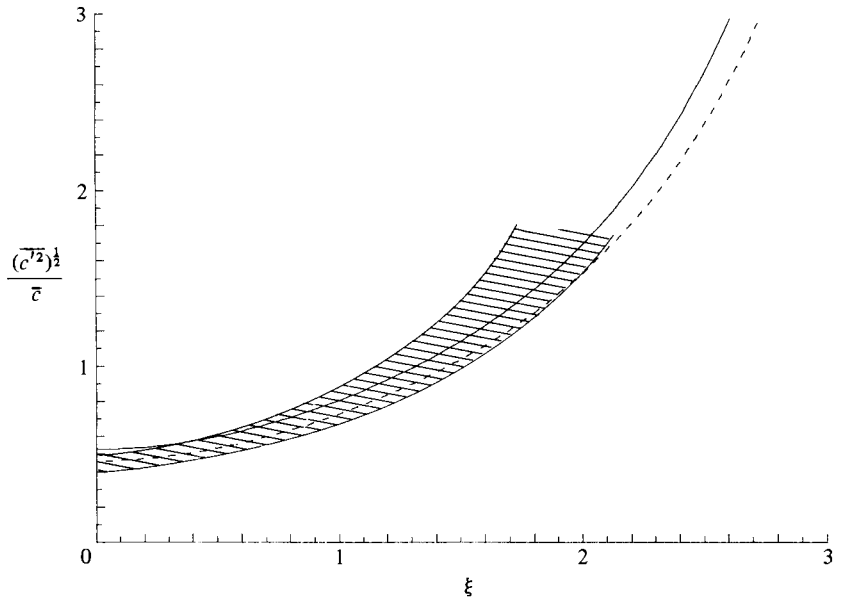

FIGURE 1. Relative intensity of concentration fluctuations $(\overline{c'^2})^{\frac{1}{2}}/\bar{c}$ as a function of dimensionless distance ξ from plume centre, for plume in decaying, isotropic turbulence. Similarity solutions for $\Gamma = 4.6$ (solid line) and $\Gamma = 5.2$ (dashed line) are shown. Shaded region indicates data of Gad-el-Hak & Morton (1979).

where z_s is the height of the source, and H is the depth of the boundary layer. The specification of the turbulence scale is discussed more fully in §3, but it should be noted that the constants α_1, α_2 etc. do have a weak dependence on the value of Λ. The initial value for σ_y is somewhat arbitrary, because the initial development of the plume is affected by such factors as turbulence in the source jet, and jet exit velocity profiles, which are ignored in the model. We are therefore beginning the integration at some effective downstream distance where the plume has grown slightly, and setting $\sigma_y = \frac{1}{2}d_s$ allows an acceptably accurate fit to the data points, as we shall show below. We have not varied this parameter in the optimization procedure, so it is possible that there is a better effective source size for this experiment.

The integrations were made on a finite-difference grid that expands with the plume to maintain similar resolution at all times. Spatial differences were second-order-centred, and the time-differencing scheme utilized the ADI method. Fields were interpolated linearly onto the new grid after expansion, and different grids and expansion rates were tested to ensure that numerical errors were insignificant. The principal comparison was with $\hat{c}/C_m$, where $\hat{c}^2$ is the maximum value of $\overline{c'^2}$, and C_m is the maximum $\bar{c}$ at any x-station. Various combinations of α_1, α_2 were tested, and a good fit to the measurements was obtained with $\alpha_1 = 0.34$, $\alpha_2 = 0.54$. The results for this combination are shown in figure 2, together with the observations of Fackrell & Robins. The model gives a good fit to all the data points; in particular, the variation with source size is accurately described, confirming the correctness of the form for Λ_c and ϵ_c. These values of α_1 and α_2 imply $c_0 = 0.41$, $\beta_1 = 0.10$ and $\beta_2 = 0.40$.

Wilson, Robins & Fackrell (1982) and Wilson, Fackrell & Robins (1982) obtained good fits to this laboratory data also, using a largely empirical model for $\overline{c'^2}$ and

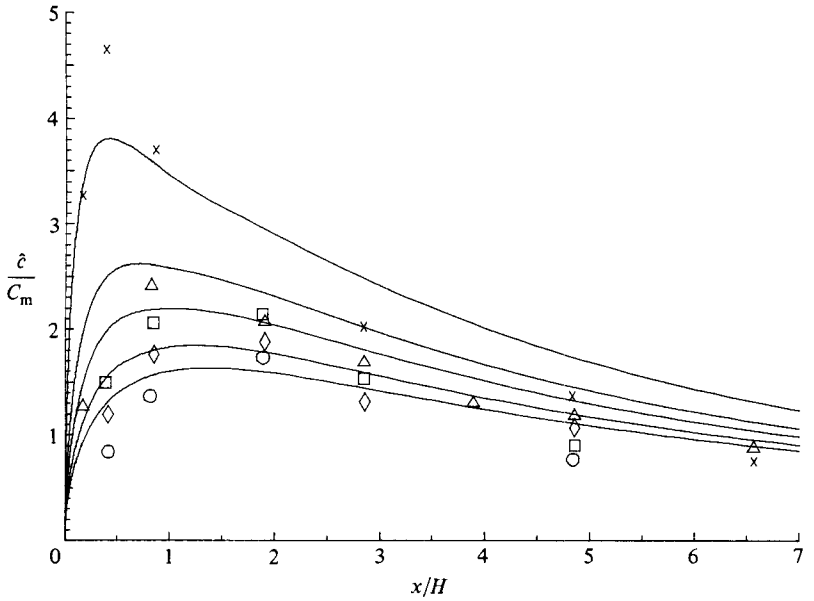

FIGURE 2. Dimensionless fluctuation intensity $\hat{c}/C_m$, for the elevated releases of Fackrell & Robins (1982*a*). Model predictions shown as solid lines for different source sizes. Symbols represent observed data as follows: ×, $d_s = 3$ mm; △, 9 mm; □, 15 mm; ◇, 25 mm; ○, 35 mm.

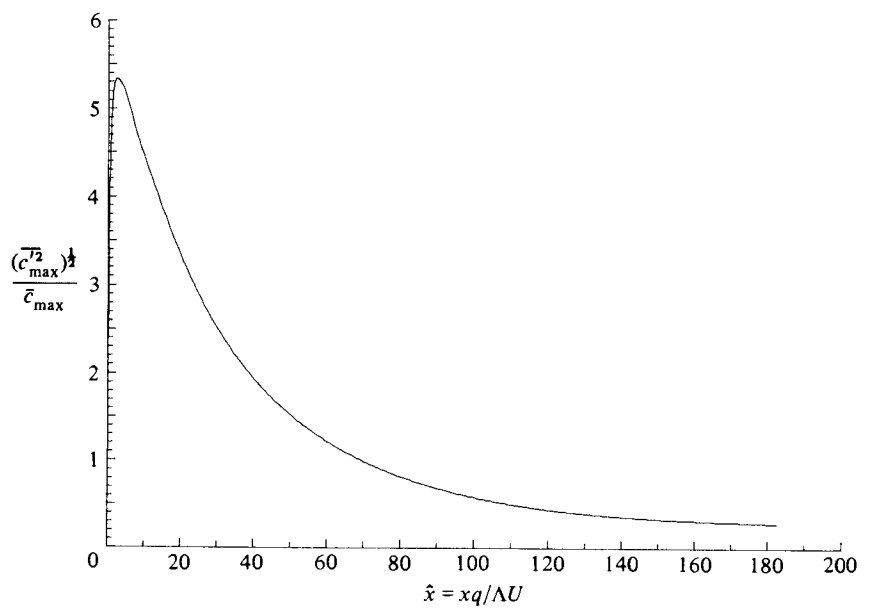

FIGURE 3. $(\overline{c'^2_{max}})^{\frac{1}{2}}/\bar{c}_{max}$ versus $xq/\Lambda U$ for release in homogeneous isotropic turbulence; $d_s/\Lambda = 0.01$.

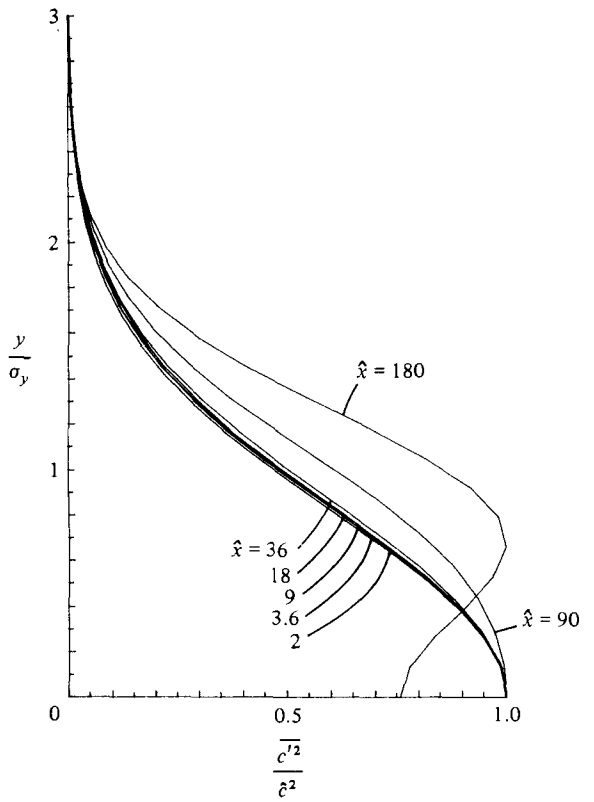

FIGURE 4. Transverse profiles of $\overline{c'^2}/\hat{c}^2$ at various downstream locations for $d_s/\Lambda = 0.01$.

suitably chosen constants. The objective of using a more complicated model here is to increase the generality by including more fundamental physics, so that a wider range of flow conditions and source sizes can be simulated.

In order to provide clearer justification of our assumption that the $\overline{c'^2}$ profile is Gaussian in the early stages, the results from an integration with $d_s/\Lambda = 0.01$ are presented here in detail. The development of $(\overline{c'^2_{max}})^{\frac{1}{2}}/\bar{c}_{max}$ (where max denotes the maximum at a downstream location) is shown in figure 3 as a function of dimensionless downstream distance $xq/\Lambda U$. The dimensionless profiles of $\overline{c'^2}$ across the plume are shown in figure 4. It is clear that the early profiles all have the same shape, which is actually Gaussian, but this eventually changes to a profile with a minimum in the centre. Comparison with figure 3 shows that the Gaussian shape begins to change where $(\overline{c'^2_{max}})^{\frac{1}{2}}/\bar{c}_{max}$ falls below about 1. This behaviour is consistent with our earlier ideas about the development of $\overline{c'^2}$ where we assumed that $\overline{c'^2}$ would be Gaussian whenever the production could be neglected. The one-half term on the left-hand side of (A 4) in the Appendix represents the production term in the $\overline{c'^2}$ equation, so this should be compared to $(\overline{c'^2_{max}})^{\frac{1}{2}}/\bar{c}_{max}$ to determine its importance, and a value of 1 is a reasonable estimate of the point where production is significant. At late times $\Lambda_c \propto t^{\frac{1}{2}}$, so the dissipation timescale is also proportional to $t^{\frac{1}{2}}$. A balance of production and dissipation at late times gives $\overline{c'^2}/\bar{c}^2 \sim t^{-\frac{1}{2}}$, and also gives a profile shaped like the gradient of $\bar{c}$, i.e. zero in the centre and maxima away from the centre. The predicted behaviour of $(\overline{c'^2_{max}})^{\frac{1}{2}}/\bar{c}_{max} \sim t^{-\frac{1}{4}}$ is a very slow decay, and is consistent with

the numerical solutions which show both slow decay of the relative intensity of the fluctuations and also a very slow transition toward the asymptotic profile shape.

As a final justification for our model for the late-time behaviours (2.11) and (2.12), Durbin's (1980) random-walk solution for a constant mean scalar gradient in homogeneous non-decaying turbulence gives $\overline{c'^2} \propto t^{\frac{1}{2}}$ at late times. Our model predicts the same dependence since Λ_c will grow like $t^{\frac{1}{2}}$, giving a dissipation timescale proportional to $t^{\frac{1}{2}}$; the scalar flux will be a constant in the presence of a constant gradient, so the production of $\overline{c'^2}$ is constant. The resulting balance between production and dissipation gives $\overline{c'^2} \propto t^{\frac{1}{2}}$. In contrast, the second-order closure model of Newman *et al.* (1981) gives $\overline{c'^2} \propto t$ and $\epsilon_c \to 0$.

3. Diffusion in non-homogeneous turbulence

Since all practical cases of interest involve non-homogeneous turbulence fields, we must consider the extension of our model to cover such cases. In air-pollution studies, the situation is generally a release within a boundary layer, so that we must deal with variations in mean velocity, turbulence energy and also turbulence lengthscales, since the latter tend to zero on the rigid boundary. The laboratory data of Fackrell & Robins (1982*a*, *b*) is very relevant to these studies and extensive comparison with our model predictions will be made. Fackrell & Robins made detailed measurements of turbulent correlations for elevated and ground releases in a wind-tunnel boundary layer, so that the performance of the model can be directly assessed from such comparisons.

In non-homogeneous turbulence, we need to account for spatial variation of variables such as K_{jm}, which were independent of position in the homogeneous case. When the background turbulence is not constant, the global integral of (2.5) needs to be replaced with a local integral so that we use only local similarity to relate the triple moments to the second moments. The appropriate range for such an integral would be the turbulence lengthscale Λ, which represents the size of the energy-containing eddies. Thus a more general definition of the diffusivity is

$$K_{jm}(\boldsymbol{x}) = -\frac{\iint_{D(\boldsymbol{x})} (x'_j - x_j)\,\overline{u'_m c'} + (x'_m - x_m)\,\overline{u'_j c'}\,\mathrm{d}y'\,\mathrm{d}z'}{\iint_{D(\boldsymbol{x})} (x'_j - x_j)\dfrac{\partial \bar{c}}{\partial x_j}\,\mathrm{d}y'\,\mathrm{d}z'}$$

where the domain $D(\boldsymbol{x}) = \{\boldsymbol{x}' : |\boldsymbol{x}' - \boldsymbol{x}| < \Lambda(\boldsymbol{x})\}$. Note that the integral in the denominator has been written in a form that makes a constant background value immaterial.

Unfortunately it is computationally expensive to calculate a local integral of this form at every spatial position at each timestep, and we have therefore used a simpler approximation in our calculations. The major effect of the local average in the boundary-layer flow is to limit K_{jm} near the wall where the lengthscale is small, and the fluxes are in local equilibrium. We have therefore retained the global integral in the definition of K_{jm}, but applied a local limit of the equilibrium value, $K_{jm} \leqslant \overline{u'_j u'_m}\,\Lambda/Aq$.

The concentration-fluctuation lengthscale Λ_c should also be treated as a spatial variable in non-homogeneous flow, and values of turbulence energy and lengthscale appearing in the equations for Λ_c and ϵ_c should probably be approximated by local integrals of the form suggested for $K_{jm}(\boldsymbol{x})$. However, in view of the computational

expense, we shall represent Λ_c as a constant for the entire plume. We calculate it exactly as in the homogeneous case, but whenever a value is required from the background field we use a plume average defined by

$$\phi_{\mathrm{p}} = \frac{\langle \bar{c}\phi \rangle}{\langle \bar{c} \rangle},$$

where ϕ is the field to be averaged. Thus (2.8) becomes

$$q_c = (q^2)_{\mathrm{p}}^{\frac{1}{2}} \left(\frac{\Lambda_c}{\Lambda_{\mathrm{p}}}\right)^{\frac{1}{3}} \quad (\Lambda_c \ll \Lambda_{\mathrm{p}}),$$

for example.

A similar philosophy also lies behind our neglect of mean strain and surface-reflection terms in the pressure-gradient correlations appearing in the scalar flux equations. Complicated models exist which claim to model these effects (e.g. Gibson & Launder 1978), but their accuracy and generality have not been proven; we therefore prefer to retain the simplest model until the need for a better representation is demonstrated. We note that the scalar variance equation does not contain any pressure terms, and is thus unaffected by this modelling choice.

There is one further extension which we found necessary but less obvious. This involves the horizontal concentration flux $\overline{v'c'}$ and its behaviour near the boundary wall. If we simply use the local scales for q and Λ in the $\overline{v'c'}$ equation, then the damping timescale will vanish near the wall because $\Lambda \sim 0.65z$ (Lewellen 1977), and therefore $\overline{v'c'}$ will be $O(z)$ because the production term

$$-\overline{v'^2}\frac{\partial \bar{c}}{\partial y}$$

remains finite. Measurements by Fackrell & Robins (1982*a*) show that $\overline{v'c'} = O(\ln z)$ near the wall, as can be seen from their figure 18, which shows $\overline{v'c'}/\bar{U}(z)$ remaining constant as $z \to 0$. Fackrell & Robins' interpretation of this measurement is that the damping timescale for $\overline{v'c'}$ is proportional to $\bar{U}(z)$ near the wall, since they also show that there is a balance between production and damping in this region. They note that the behaviour of $\overline{v'c'}$ is precisely that required to ensure that the plume spreads laterally at the same rate at all heights, the rate being measured as a function of distance x downstream from the source. There seems to be no rationale for a turbulent timescale that varies like $\bar{U}(x)$, and we therefore propose a different physical model for the observed behaviour. Our hypothesis is based on our view of the plume as a coherent entity, so that concentration fluctuations occur on the same lengthscale throughout the plume. We suggest that there are therefore contributions to $\overline{v'c'}$ on the scale Λ_{p}, i.e. the average turbulence scale over the plume. Note that this is not the fluctuation scale Λ_c, but is the scale of the average turbulent eddies that are diffusing the plume. This scale will be considerably larger than the local scale near the wall if the plume extends significantly upward from the boundary. Such a scale is prohibited in the vertical flux $\overline{w'c'}$, since the proximity of the wall prevents any large scales in the vertical direction. Assuming that there are contributions to $\overline{v'c'}$ on the Λ_{p} scale, we can then explain the observations by pointing out that the production term

$$-\overline{v'^2}\frac{\partial \bar{c}}{\partial y}$$

occurs on the local scale Λ, because that is the scale of $\overline{v'^2}$. Thus small-scale

contributions to $\overline{v'c'}$ are produced locally, and also removed locally on the short local timescale, giving the observed balance between production and damping. There is, however, very little energy in this small-scale contribution; the main part of $\overline{v'c'}$ near the wall is in the Λ_p scale which is damped on the much slower

$$\frac{\Lambda_p}{(q^2)_p^{\frac{1}{2}}}$$

timescale, and reaches the ground via diffusion from above. Thus vertical coupling of $\overline{v'c'}$ is the factor that ensures that the plume diffuses at the same rate at all heights, and hence produces the observed $\overline{v'c'}$ profiles. We must determine the partition of $\overline{v'c'}$ between the two scales Λ_p and Λ within the model, because the assumption that $\overline{v'c'}$ is all on the Λ_p scale would give $\overline{v'c'}$ tending to a constant value at the wall rather than proportional to $\bar{U}(z)$. We propose a crude but simple estimate based on the local production rate of $\overline{v'c'}$, namely

$$\overline{v'c'_s} = \frac{-\overline{v'^2}\Lambda}{Aq}\frac{\partial \bar{c}}{\partial y}, \tag{3.1}$$

where $\overline{v'c'_s}$ is the small-scale contribution to $\overline{v'c'}$, with the restriction that

$$0 \leqslant \frac{\overline{v'c'_s}}{\overline{v'c'}} \leqslant 1.$$

Equation (3.1) postulates a balance between small-scale production and dissipation whenever possible, but does not allow the small-scale dissipation to exceed the small-scale production. Defining $\overline{v'c'_p} = \overline{v'c'} - \overline{v'c'_s}$, we write the damping term in the $\overline{v'c'}$ equation as

$$-\frac{Aq}{\Lambda}\overline{v'c'_s} - \frac{A(q^2)_p^{\frac{1}{2}}}{\Lambda_p}\overline{v'c'_p}. \tag{3.2}$$

This model implies that when larger values of $\overline{v'c'}$ are present near the ground than could be produced by the local turbulence, presumably by diffusion from aloft, then the additional $\overline{v'c'}$ is dissipated on the longer average plume timescale. We show model results below which indicate that this crude parametrization gives reasonably good predictions of the $\overline{v'c'}$ profiles.

Finally, in accord with the above philosophy, we calculate the horizontal diffusivities in the modelled triple correlation terms using plume-average quantities rather than local values. This is not strictly justified since we have postulated only part of the correlations on the Λ_p scale, but the differences from calculating each part separately do not justify the extra complexity, since diffusion is usually unimportant when the small-scale contribution is dominant.

We are now in a position to compare our model predictions with the data obtained by Fackrell & Robins. In order to ensure that we are evaluating the predictions of the scalar transport equations, we use the measured profiles for the dynamical quantities rather than a model prediction. Unfortunately, the turbulence lengthscale Λ is not easily specified from the measurements. Λ is used to determine several different timescales in the model, with coefficients which have been determined to be consistent with other model predictions. We lose this consistency by using measured values for the Reynolds stress, so that Λ becomes somewhat arbitrary. Rather than use the measured dissipation rate to set Λ, we chose a simple algebraic form which is consistent with earlier model integrations for boundary-layer flows (Lewellen 1977), namely

$$\frac{1}{\Lambda} = \frac{1}{0.65z} + \frac{1}{0.2H}, \tag{3.3}$$

where H is the boundary-layer thickness. The linear relation is appropriate near the wall, while the constant value is a typical value in the outer part of the boundary layer; the latter value is also roughly consistent with the dissipation measurements of Fackrell & Robins for $z/H = 0.5$. We may note that the integrations reported below were also run with a different scale profile between the two limits, namely

$$\Lambda = \min(0.65z, 0.2H), \tag{3.4}$$

and produced results which were in most cases within 15% of those presented. In making these runs, α_1 and α_2 were set to 0.30 and 0.56 to optimize the fit with the elevated release data using the different value for Λ implied by (3.4).

We have also used $4\overline{w^2}$ in place of q^2 in all the modelled terms, because the observed q^2 implies inconsistent behaviour of the effective diffusivity in the surface layer. This was one of the means for determining model constants (Lewellen 1977), so that consistency here is quite important. We note that the observed profile of $\overline{w^2}$ is very close to the model predictions, and the model surface-layer relationship $q^2 = 4\overline{w^2}$ allows us to make a consistent estimate of q^2 from the observations.

Having defined all the background turbulence fields, and the evolution equations for the scalar quantities, the parabolic equations were integrated in a two-dimensional domain, marching in the streamwise direction, i.e.

$$\frac{\mathrm{D}}{\mathrm{D}t} = \bar{U}(z)\frac{\partial}{\partial x}.$$

At the lower boundary $z = 0$ we specify the appropriate conditions for an impenetrable wall, i.e.

$$\frac{\partial \bar{c}}{\partial z} = \overline{c'w'} = \frac{\partial}{\partial z}\overline{c'v'} = \frac{\partial}{\partial z}\overline{c'^2} = 0. \tag{3.5}$$

All scalar quantities are set to zero on the outer boundaries $z = Z_\mathrm{m}$ and $y = Y_\mathrm{m}$, and we use a plane-of-symmetry condition at $y = 0$ so that only half the domain needs to be considered. The outer boundaries Y_m, Z_m are adjusted during the integration to maintain

$$Y_\mathrm{m} \in [7\sigma_y, 10\sigma_y], \quad Z_\mathrm{m} \in [\bar{z} + 14\sigma_z, \bar{z} + 20\sigma_z],$$

where $\bar{z}$ is the height of the plume centroid, and σ_y and σ_z are the plume spreads.

Integrations were made for all the cases reported by Fackrell & Robins; these constitute five elevated releases and three ground releases. Detailed profiles for the 9 mm elevated release and the 15 mm ground release are reported, while the ratio of concentration fluctuation standard deviation to mean concentration are given for all the releases. We first compare the model predictions for the latter quantities, giving some overall comparison of the model performance on the range of data.

Figure 5 shows the model predictions for the ratio of the maximum value of $(\overline{c'^2})^{\frac{1}{2}}$ $(= \hat{c})$ to the maximum value of $\bar{c}$, denoted by C_m, as a function of x/H. The data of Fackrell & Robins are also displayed in the figure. The elevated releases are little different from the homogeneous results shown in figure 1, as anticipated in §2. The ground releases show reasonable agreement with the measurements also, although they lie somewhat below the virtually constant observed value of 0.6 over the range of release diameters and over the downstream range of the data. Figure 5 demonstrates the ability of the model to predict the independence of the ratio of standard deviation to mean for a wide range of releases.

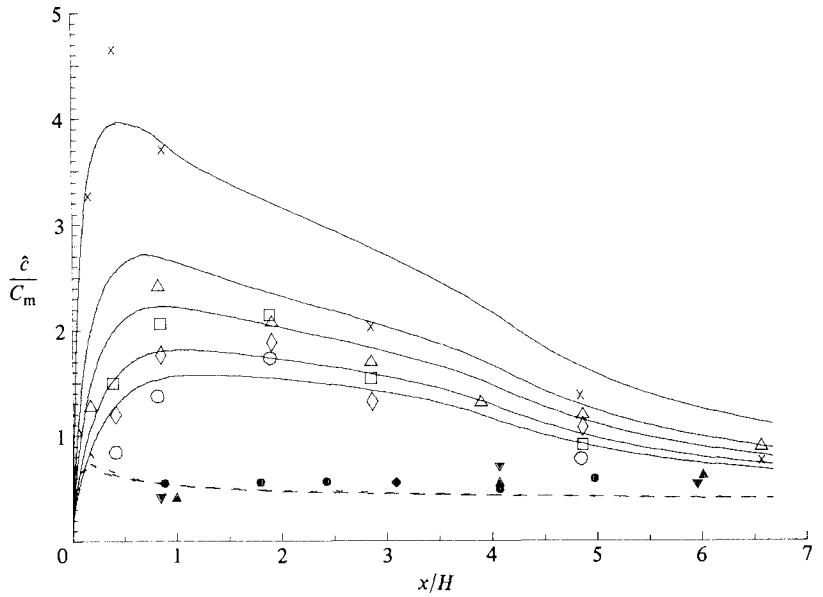

FIGURE 5. Full model predictions for $\hat{c}/C_m$ in elevated and ground releases. Symbols as in figure 2 for elevated releases. Ground-release predictions are shown as dashed lines, data symbols are △, 3 mm; ▽, 9 mm; ○, 15 mm.

It is true that two empirical constants were chosen to optimize the fit for the elevated releases, but the agreement with measurements on the shape and magnitude of the range of data values strongly suggests that the dominant physical processes and timescales have been incorporated into the model. Further support for this view comes from examination of the detailed measurements of the plumes.

Figure 6 shows the evolution of several plume quantities, namely C_m, δ_y and δ_z for the elevated (9 mm) and ground (15 mm) releases. δ_y and δ_z are the plume scales, defined by Fackrell & Robins as the distance over which the concentration falls to half its maximum value. In the y-direction, the plume shapes are very close to Gaussian, so we have plotted $\delta_y = 1.17\sigma_y$, which is the appropriate value. For the ground release the vertical profiles are nearly self-similar, as we shall see below, so that δ_z is defined from the profile at $y = 0$. For the elevated release, however, Fackrell & Robins obtained δ_z by fitting a reflected Gaussian to the measured profile and relating δ_z to the Gaussian spread. Since a Gaussian does not provide a good fit at late times, we have simply plotted $\delta_z = 1.17\sigma_z$, where σ_z is the standard deviation of the entire plume, i.e. no reflections considered. This should agree with the measurements at early times, but is a different measure after the plume has touched the ground, so that the comparison is not useful after $x/H = 3$ in figure 6(*b*). The maximum concentration on the ground is also shown in figure 6(*b*). The predictions of the spread rates and maximum concentrations are generally good for both releases. There is a tendency to underpredict the horizontal spread rate for the ground release by about 20 %, with a consequent 20 % overprediction of the maximum concentration. The elevated release is predicted accurately until it reaches the ground, where the diffusion is too slow. The latter point will be discussed further when we examine the profile shapes.

Comparisons of the shape of the concentration profiles (normalized by the

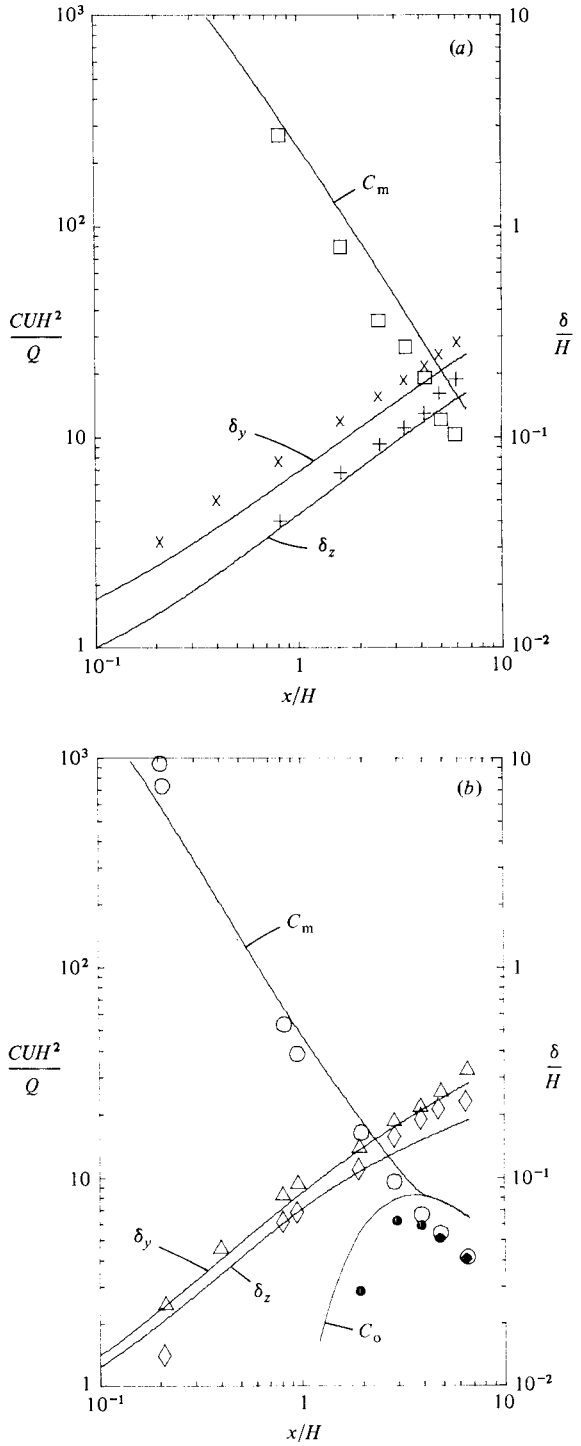

FIGURE 6. Predictions and observations of plume spread and maximum concentrations. Predictions shown as solid lines. (*a*) Ground release; data: □, C_m; +, δ_z; ×, δ_y. (*b*) Elevated release; data: ○, C_m; ■, C_0; ◇, δ_z; △, δ_y (C_0 is the maximum concentration on the surface).

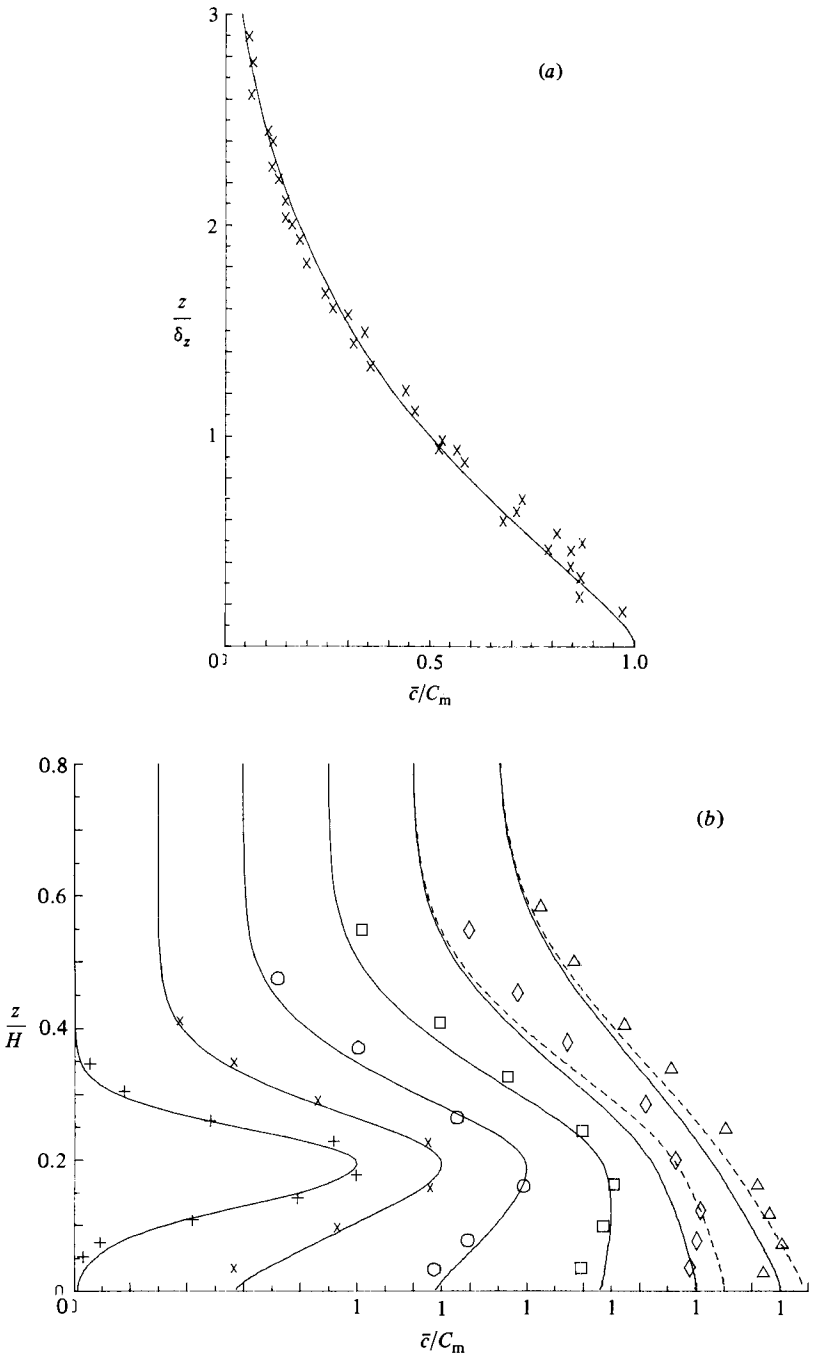

FIGURE 7. Vertical profiles of $\bar{c}/C_m$ at plume centre. (*a*) Ground release. (*b*) Elevated release; data symbols: +, $x/H = 0.96$; ×, 1.92; ○, 2.88; □, 3.83; ◇, 4.79; △, 6.52. Note that origins of consecutive profiles are offset to the right.

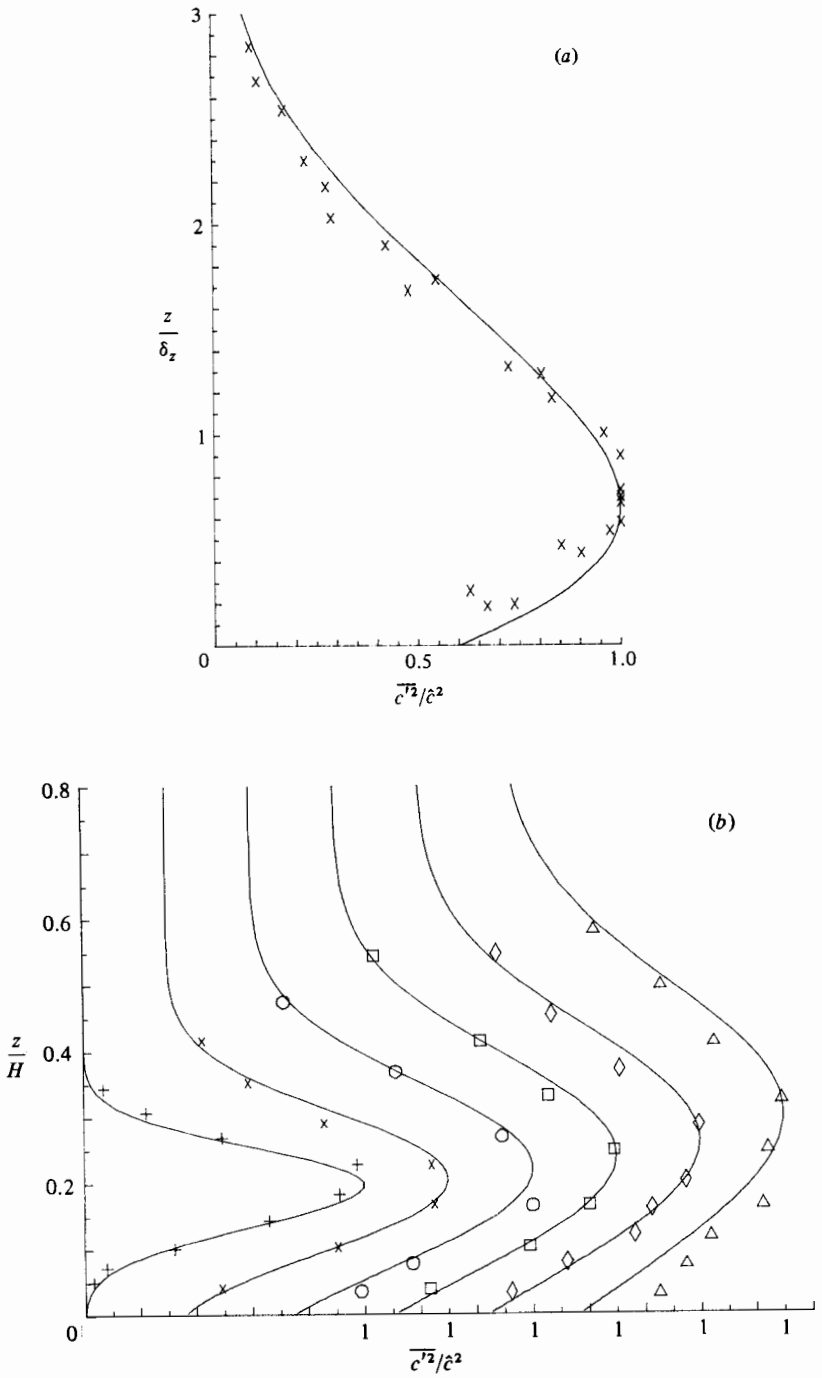

FIGURE 8. Vertical profiles of $\overline{c'^2}/\hat{c}^2$. Symbols as figure 7. (*a*) Ground release. (*b*) Elevated release.

maximum concentration) in the vertical direction are shown in figure 7. The ground-level release profiles collapsed onto a single non-dimensional curve when plotted against z/δ_z. Fackrell & Robins report the same results from their measurements, and the model prediction for the shape of the profile is in excellent agreement with the observations. Good results are also obtained for the elevated release, with profiles closely matching the data, except for the latest station which indicates the model prediction progressing toward the final ground-release shape more quickly than the observations. The discrepancies are only significant very close to the ground, as the dashed lines in figure 7 (*b*) demonstrate. These profiles were obtained by rescaling $\bar{c}$ so that the actual maximum is predicted correctly; those curves are different because the observed maximum is elevated whilst the model predicts the maximum on the ground. It is evident that the upper region of the profile is more accurately predicted. The errors below $z/H = 0.1$ are probably due to underprediction of the horizontal fluxes near the ground, as we shall see later. We note however, that there seems to be some inconsistency in the data near the ground also; figure 6 (*b*) shows the observed maximum to be on the ground at the last station, while figure 7 (*b*) shows the ground value to be significantly lower than the maximum.

The model profiles are the most sensitive to changing the specification of Λ; use of (3.4) causes the elevated release to diffuse downward and develop the features of the ground release more quickly, although the differences are still less than about 25 %.

We also compare the vertical profiles of $\overline{c'^2}$, again normalized by the maximum value in the profile; the results are shown in figure 8. The ground release profiles collapse onto a self-similar curve when plotted against δ_z; this curve shows a maximum value of $\overline{c'^2}$ at about $0.75\delta_z$, with reduction to about half the maximum value at the surface. The model prediction is very close to the measurements again.

For the elevated release (figure 8*b*) there is also good agreement with observation. At early times the $\overline{c'^2}$ profile is close to Gaussian, as discussed in §2 for homogeneous turbulence. As the Gaussian spreads, it eventually reaches the ground plane and ceases to mirror the mean concentration profile. Instead, $\overline{c'^2}$ remains small near the ground, and the elevated maximum begins to move upward, following the region of maximum production where gradients of $\bar{c}$ are significant.

The second-order closure model predicts the observed reduction in $\overline{c'^2}$ near the wall, which Fackrell & Robins suggest arises through increased dissipation by the small eddies in that region. The model, however, does not include such a mechanism because we have assumed that the concentration fluctuations occur principally on the Λ_c scale. There is a slight increase in the dissipation rate near the wall due to the increase in turbulence energy, but this is only a small effect. The main cause of the small $\overline{c'^2}$ seems to be the absence of production terms; we plotted the profile on the centreline, $y = 0$, so that $\overline{v'c'} = 0$ at all heights, and also $\overline{w'c'} = 0$ on the lower boundary. Thus there is no production of $\overline{c'^2}$ at the ground, and the value there is determined by the rate of diffusion. The diffusion rate in the vertical is small near the ground, since the scale of the eddies with significant energy in the vertical component must tend linearly to zero at the wall and we limit the diffusivity using the local equilibrium rate; there is therefore a low value of $\overline{c'^2}$ in this region, the value being determined by the horizontal diffusion rate. The difference between the point on the ground and the point of maximum $\bar{c}$ in the early elevated plume is in the diffusion rate only, both points have no production of $\overline{c'^2}$, but the elevated point has a larger scale for the vertical eddies, and consequently diffuses $\overline{c'^2}$ much faster to fill in the region of low production.

Lateral cross-sections of $\overline{c'^2}$ illustrate the roles of diffusion and production, figure

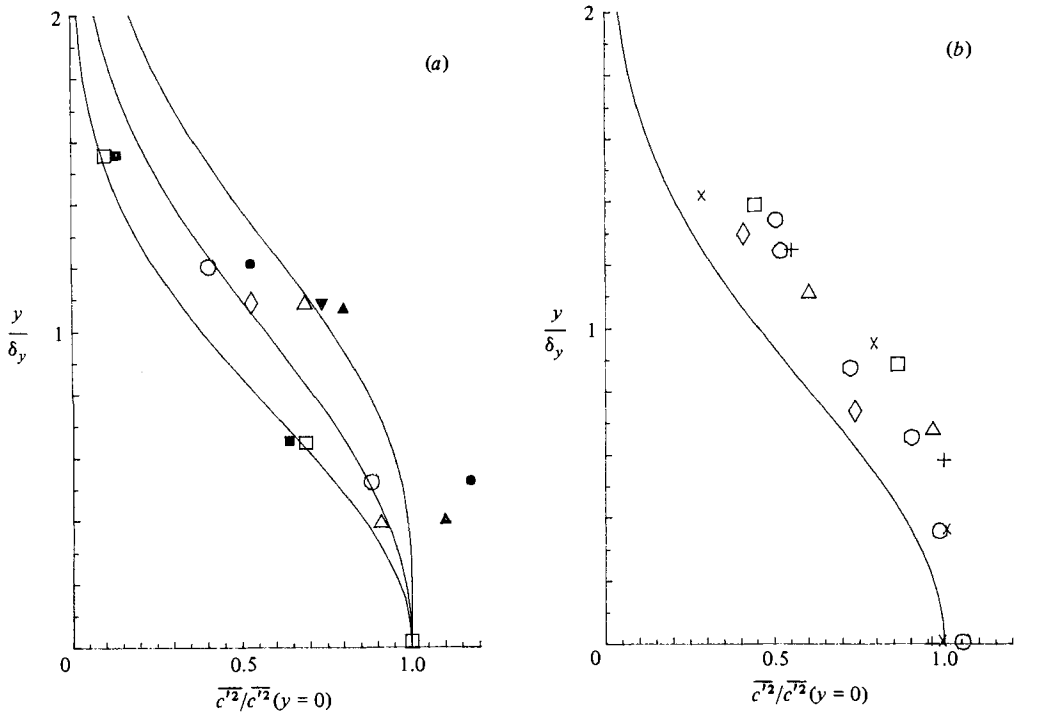

FIGURE 9. Transverse profiles of $\overline{c'^2}$. (*a*) Ground release; solid data symbols are at $z/\delta_z = 0.5$, open symbols at $z/\delta_z = 1.5$. (*b*) Elevated release; all profiles are at the height of maximum c'^2.

9(*a*) shows cross-sections through the ground release at three different heights. The curves are the same at all x-stations when normalized by δ_y and the centreline value. We may note that the mean-concentration profiles are all close to Gaussian in the y-direction, in accord with observations, and the spread measured at various heights is generally within 10 % of the mean value obtained for the entire plume. Figure 9(*a*) shows the model predicting a very slight minimum on the centreline at $z = 0$, but a maximum on $y = 0$ at $z = \frac{1}{2}\delta_z$ and $z = \frac{3}{2}\delta_z$. The measured profiles at the two elevated positions show a relatively lower value at $y = 0$, i.e. more tendency toward a minimum on the centreline; the measured profile at $z = \frac{1}{2}\delta_z$ is closer to the predicted profile at $z = 0$. The model has the correct quantitative behaviour, but details of the profile shapes are not precise. We believe that the discrepancies here are due to errors in $\overline{v'c'}$ near the ground, and consequent errors in the production rate for $\overline{c'^2}$; the flux profiles will be discussed in detail below. The profiles for the elevated release at the height of the maximum $\overline{c'^2}$ are shown in figure 9(*b*); these also agree quite well with the observations, but show the same tendency as the ground release to be closer to Gaussian than the observation.

Normalized vertical profiles of the vertical concentration flux $\overline{w'c'}$ are shown in figures 10 and 11. Figure 10 shows ground-release results for two downstream stations, and various positions across the plume. The centreline profile and the inner profile at roughly $y = \frac{1}{2}\delta_y$ from the model prediction collapse together very well, but the outer profile at $y \geqslant \delta_y$ is slightly larger in magnitude, with a sharper maximum. The measured profiles do not really confirm this change in profile, but there are generally higher values in the outer profile. The overall agreement in profile shape

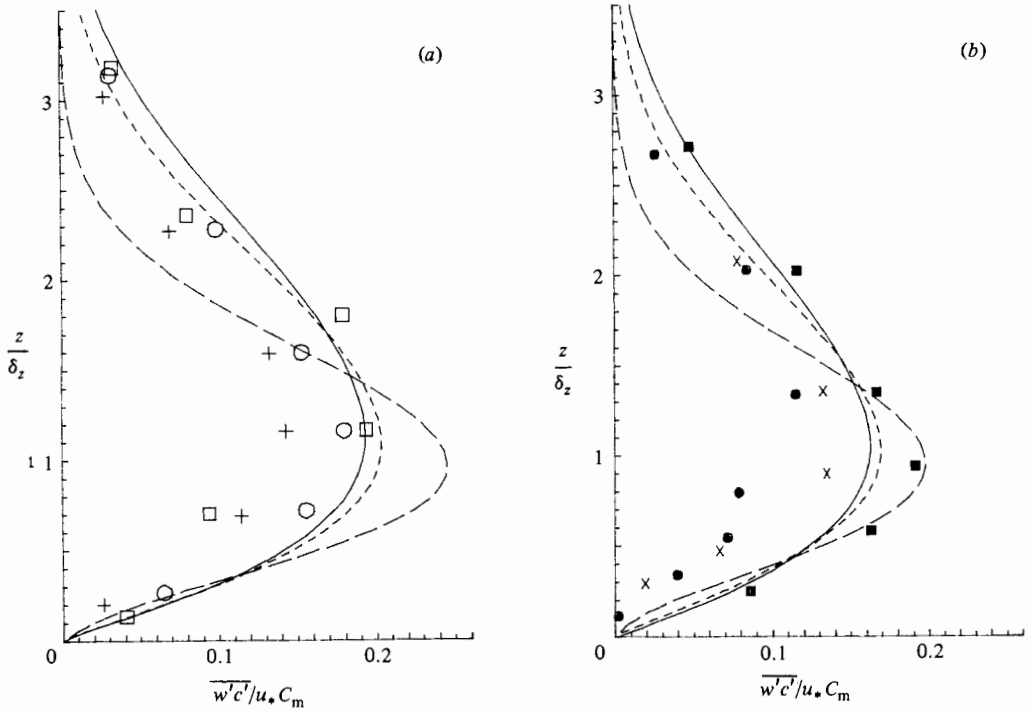

FIGURE 10. Vertical profiles of vertical flux $\overline{w'c'}$ for the ground release.

(a) $x/H = 2.5$:	y/δ_y	Model	Data	(b) $x/H = 5.92$:	y/δ_y	Model	Data
	0	——	+		0	——	×
	0.39	-----	○		0.51	-----	○
	1.07	– – –	□		1.20	– – –	■

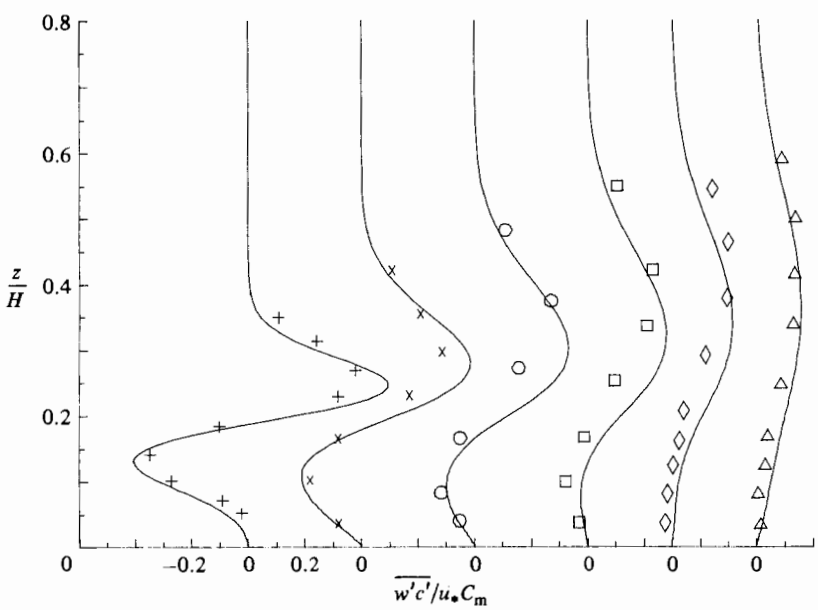

FIGURE 11. Vertical profiles of $\overline{w'c'}$ for the elevated release. Symbols as in figure 7.

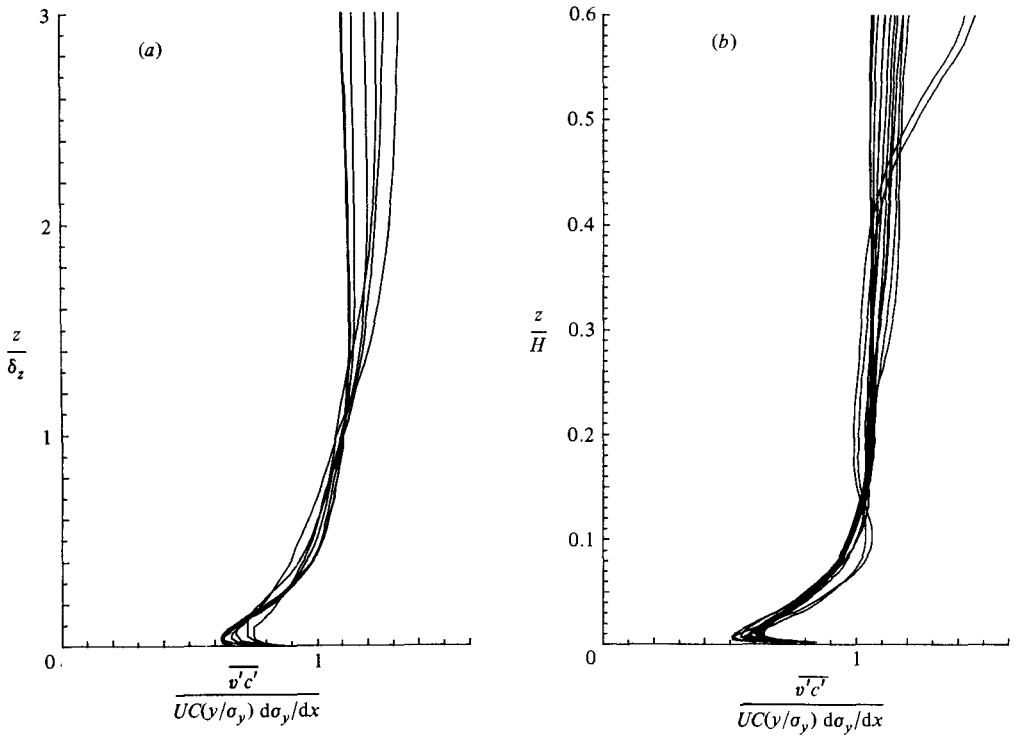

FIGURE 12. Dimensionless profiles of $\overline{v'c'}$ at the range of locations reported by Fackrell & Robins. (*a*) Ground release. (*b*) Elevated release.

is very good. The same is true of the centreline profiles for the elevated release, shown in figure 11; predicted and observed values agree very well.

Vertical profiles of the normalized lateral flux $\overline{v'c'}$ are shown in figure 12 for ground and elevated releases. The graphs are a composite of all the profiles at the positions plotted by Fackrell & Robins, which covers the range of downstream stations and also lateral position within the plume. The normalization includes the mean velocity $\bar{u}(z)$, and is the appropriate scaling (as shown by Fackrell & Robins) if the plume is diffusing laterally at the same rate at all heights. The measurements show a scatter of points within about 20 % of unity, and no evident trend with height or downstream or lateral portion. The model predictions do not show any significant trend with downstream or lateral position, but there is a reduction to a value of 0.5 at the surface, which takes the model results out of the band of the measurement below about $0.4\delta_z$ for the ground release and below $z = 0.07H$ for the elevated release.

The behaviour of $\overline{v'c'}$ near the ground was discussed at the beginning of this section, and used as the basis of a 'two-scale' model, i.e. we considered $\overline{v'c'}$ to be composed of fluctuations on two distinct scales near the ground, namely Λ_p and Λ. Our estimate of the fraction in the small scale Λ is denoted by $\overline{v'c'_s}$ and given in (3.1). We accept that this is a very crude description of the dynamics, but point out that the assumption that all the lateral flux is on one scale, i.e. $\overline{v'c'_s} = 0$ or $\overline{v'c'_s} = \overline{v'c'}$, results in significantly worse predictions of the vertical profile, and also gives a plume which diffuses at a very different rate near the ground. The two-scale description of $\overline{v'c'}$ does introduce considerable potential for complexity, but seems to be necessary to understand the behaviour of the plume. Having accepted the impossibility of

modelling the flow with a single scale, we feel justified in choosing the simplest conceptual model in order to investigate its consequences and possibilities. Although the prediction of $\overline{v'c'}$ is in error close to the ground, the discrepancies are much smaller than the one-scale model, and we have gone some way toward an accurate description of these processes.

As noted earlier, the reduced value of $\overline{v'c'}$ near the surface is probably responsible for the lateral $\overline{c'^2}$ profiles being closer to Gaussian, in that larger values of $\overline{v'c'}$ would give higher production off the centreline, and tend to increase $\overline{c'^2}$ in that region.

4. Summary and conclusions

A second-order closure model for the dispersion of a passive scalar has been presented and tested against laboratory data. The model improves upon the earlier work of Lewellen & Teske (1976) in that attention has been paid to the early stages of the release to ensure that correct behaviour is modelled. Our final model predicts the linear and parabolic regimes of the mean-concentration profile growth without any new empirical constraints, and compares well with experimental data. The main restriction is that each release must be treated separately; this seems to be a fundamental problem with any closure scheme, as shown by Deardorff (1978). However, we have removed any requirement from the specification of time-dependent diffusivities, by allowing all the turbulence correlations to diffuse at the same rate as the mean concentration in the early stages. This closes the system of equations, allowing the closure model to completely determine the solution in terms of the background turbulence parameters.

The new model also includes a prediction of the concentration variance $\overline{c'^2}$; this quantity is known to be dependent on source size, and introduces a new lengthscale into the problem, namely the concentration fluctuation scale Λ_c. A simple equation for Λ_c has been prepared which is based on the behaviour in the limits of very small or very large Λ_c. These limits are obtained by identifying Λ_c with the two-particle separation as discussed by Durbin (1980). Having determined these asymptotic behaviours, empirical coefficients were then chosen to optimize the agreement with the data of Fackrell & Robins (1982*a*). It should be noted that the shape of the $\overline{c'^2}$ evolution, as well as its variation with source size, is predicted, so that agreement does imply that the dynamics are being described correctly.

In conclusion, it has been demonstrated that the dispersion of a passive scalar can be modelled using second-order closure techniques under the idealized laboratory conditions considered in this paper. The main advantage of the closure scheme is that it provides a foundation for considering more complex situations, as well as a framework within which simpler parametrizations can be developed.

This work was partially supported by EPRI with G. R. Hilst as project manager and by NRC with R. F. Abbey as project manager.

Appendix

We examine here the early-stage model predictions for the concentration variance. Recalling that we denote the integral over the plume by angular brackets, we can combine the $\overline{c'^2}$ equation with the $\bar{c}$ equation to obtain

$$\frac{\mathrm{D}}{\mathrm{D}t}(\langle\overline{c'^2}\rangle + \langle\bar{c}^2\rangle) = -\langle\epsilon_c\rangle. \tag{A 1}$$

We know from §2.1 that $\bar{c}$ has a Gaussian profile, with standard deviations σ_y and σ_z given by $(\sigma_0 + (\overline{v^2})^{\frac{1}{2}}t)$ and $(\sigma_0 + (\overline{w^2})^{\frac{1}{2}}t)$ respectively, where σ_0 is the initial (circular) spread of the plume. If we assume that c'^2 has the same profile shape as $\bar{c}$, then (A 1) will become an equation for the centreline value of $\overline{c'^2}$. This assumption is justified by numerical solution of the full equations (see figure 2.4), but we note here that $\overline{c'^2}$ does mirror the $\bar{c}$-distribution for some time, because the production of $\overline{c'^2}$ occurs very early during the release from a small source. Once the production phase is passed, $\overline{c'^2}$ diffuses at the same rate as $\bar{c}$, by construction, and therefore will adopt the same Gaussian profile.

If $\hat{c}^2$ and C_m are the centreline values of $\overline{c'^2}$ and $\bar{c}$ respectively, then (A 1) can be rewritten as

$$\frac{\mathrm{D}}{\mathrm{D}t}(\sigma_y \sigma_z [\hat{c}^2 + \tfrac{1}{2}C_\mathrm{m}^2]) = -\frac{\alpha_2 q_c}{\Lambda_c}\sigma_y \sigma_z \hat{c}^2. \tag{A 2}$$

Equations (2.8) and (2.9) can be solved to give

$$\Lambda_c = [\sigma_0^{\frac{2}{3}} + \tfrac{2}{3}\alpha_1 qt\Lambda^{-\frac{1}{3}}]^{\frac{3}{2}}, \tag{A 3}$$

where we set $\Lambda_c(0) = \sigma_0$. We have the freedom to set this initial condition since we allowed two empirical constants in the earlier equations.

Substituting for σ_y and σ_z, and using the fact that the total flux $C_\mathrm{m}\sigma_y\sigma_z$ is conserved, (A 2) becomes

$$\frac{\mathrm{D}}{\mathrm{D}t}\left(\sigma_y^{-1}\sigma_z^{-1}\left[\frac{\hat{c}^2}{C_\mathrm{m}^2} + \frac{1}{2}\right]\right) = -\frac{\alpha_2 q}{\sigma_0^{\frac{2}{3}}\Lambda^{\frac{1}{3}} + \frac{2}{3}\alpha_1 qt}\sigma_y^{-1}\sigma_z^{-1}\frac{\hat{c}^2}{C_\mathrm{m}^2}, \tag{A 4}$$

where the equation has been written in terms of the variable $\hat{c}/C_\mathrm{m}$, which measures the relative intensity of the concentration fluctuations. For a small source ($\sigma_0/\Lambda \ll 1$) $\hat{c}/C_\mathrm{m}$ will be large, so the term in square brackets on the left-hand side of (A 4) is approximately $\hat{c}^2/C_\mathrm{m}^2$. However, the one-half cannot be neglected in the very early stages, since it represents the production terms. The production can be seen to be important only for $t < \sigma_0/q$, by which time $\hat{c}/C_\mathrm{m}$ is $O(1)$; this is a very short time and justifies our Gaussian assumption. Hence for $t > O(\sigma_0/q)$ (A 4) predicts a relatively straightforward decay of $(\sigma_y\sigma_z)^{-1}\hat{c}^2/C_\mathrm{m}^2$.

The solution is

$$\frac{\hat{c}^2}{C_\mathrm{m}^2} = \frac{A_0}{\sigma_0^2}\sigma_y\sigma_z\left[1 + \tfrac{2}{3}\alpha_1\frac{qt}{\sigma_0^{\frac{2}{3}}\Lambda^{\frac{1}{3}}}\right]^{-\gamma}, \tag{A 5}$$

where $\gamma = 3\alpha_2/2\alpha_1$, and A_0 is an $O(1)$ constant related to the maximum value of $\hat{c}^2$ attained at the end of the production phase.

Several features can be noted from (A 5). First, $\hat{c}/C_\mathrm{m}$ will only maximize within this early-time solution if $\gamma > 2$, since σ_y and σ_z grow linearly with t for t much smaller than the turbulence time Λ/q; this imposes a constraint on the empirical constants α_1 and α_2. Secondly, if $\gamma > 2$ the maximum $\hat{c}/C_\mathrm{m}$ occurs at $t = O(\sigma_0^{\frac{2}{3}}\Lambda^{\frac{1}{3}}/q)$ and takes a value $O(\Lambda^{\frac{1}{3}}/\sigma_0^{\frac{1}{3}})$.

REFERENCES

Antonopoulos-Domis, M. 1981 Large-eddy simulation of a passive scalar in isotropic turbulence. *J. Fluid Mech.* **104**, 55–79.

Chatwin, P. C. & Sullivan, P. J. 1979*a* The relative diffusion of a cloud of passive contaminant in incompressible turbulent flow. *J. Fluid Mech.* **91**, 337–355.

Chatwin, P. C. & Sullivan, P. J. 1979*b* Measurements of concentration fluctuations in relative turbulent diffusion. *J. Fluid Mech.* **94**, 83–101.

CHATWIN, P. C. & SULLIVAN, P. J. 1980 Some turbulent diffusion invariants. *J. Fluid Mech.* **97**, 405–416.

CSANADY, G. T. 1967 Concentration fluctuations in turbulent diffusion. *J. Atmos. Sci.* **24**, 21–28.

DEARDORFF, J. W. 1978 Closure of second- and third-moment rate equations for diffusion in homogeneous turbulence. *Phys. Fluids* **21**, 525–530.

DONALDSON, C. DUP. 1973 Atmospheric turbulence and the dispersal of atmospheric pollutants. In *Proc. AMS Workshop on Micrometeorology* (ed. D. A. Haugen). Science Press, Boston.

DURBIN, P. A. 1980 A stochastic model of two-particle dispersion and concentration fluctuations in homogeneous turbulence. *J. Fluid Mech.* **100**, 279–302.

DURBIN, P. A. 1982 Analysis of the decay of temperature fluctuations in isotropic turbulence. *Phys. Fluids* **25**, 1328–1332.

EL TAHRY, S., GOSMAN, A. D. & LAUNDER, B. E. 1981 The two- and three-dimensional dispersal of a passive scalar in a turbulent boundary layer. *Intl J. Heat Mass Transfer* **24**, 35–46.

FACKRELL, J. E. & ROBINS, A. G. 1982*a* Concentration fluctuations and fluxes in plumes from point sources in a turbulent boundary layer. *J. Fluid Mech.* **117**, 1–26.

FACKRELL, J. E. & ROBINS, A. G. 1982*b* The effects of source size on concentration fluctuations in plumes. *Boundary-Layer Met.* **22**, 335–350.

GAD-EL-HAK, M. & MORTON, J. B. 1979 Experiments on the diffusion of smoke in isotropic turbulent flow. *AIAA J.* **17**, 558–562.

GIBSON, M. & LAUNDER, B. E. 1978 Ground effects on pressure fluctuations in the atmospheric boundary layer. *J. Fluid Mech.* **67**, 569–581.

GIFFORD, F. 1959 Statistical properties of a fluctuating plume dispersal model. *Adv. Geophys.* **6**, 117–137.

HAY, J. S. & PASQUILL, F. 1959 Diffusion from a continuous source in relation to the spectrum and scale of turbulence. *Adv. Geophys.* **6**, 345–365.

LAUNDER, B. E., REECE, G. J. & RODI, W. 1975 Progress in the development of a Reynolds-stress turbulence closure. *J. Fluid Mech.* **67**, 537–566.

LESLIE, D. C. 1973 *Developments in the Theory of Turbulence.* Oxford University Press.

LEWELLEN, W. S. 1977 Use of invariant modelling. In *Handbook of Turbulence* (ed. W. Frost & T. M. Moulden). Plenum.

LEWELLEN, W. S. 1981 Modelling the lowest 1 km of the atmosphere. *AGARD*-AG-267.

LEWELLEN, W. S. & TESKE, M. E. 1976 Second-order closure modelling of diffusion in the atmospheric boundary layer. *Boundary-Layer Met.* **10**, 69–90.

LUMLEY, J. L. & KHAJEH-NOURI, B. 1974 Computational modelling of turbulent transport. In *Proc. 2nd IUGG–IMIAM Symp. on Atmospheric Diffusion in Environmental Pollution.* Academic.

MURTHY, C. R. & CSANADY G. T. 1971 Experimental studies of relative diffusion in Lake Huron. *J. Phys. Oceanogr.* **1**, 17–24.

NEWMAN, G. R. & HERRING, J. R. 1979 A test field model study of passive scalar in isotropic turbulence. *J. Fluid Mech.* **94**, 163–194.

NEWMAN, G. R., LAUNDER, B.E. & LUMLEY, J. L. 1981 Modelling the behaviour of homogeneous scalar turbulence. *J. Fluid Mech.* **111**, 217–232.

SAWFORD, B. L. 1982 Comparison of some different approximations in the statistical theory of relative dispersion. *Q. J. R. Met. Soc.* **108**, 191–208.

SMITH, F. B. & HAY, J. S. 1961 The expansion of clusters of particles in the atmosphere. *Q. J. R. Met. Soc.* **87**, 89–91.

TAYLOR, G. I. 1921 Diffusion by continuous movements. *Proc. Lond. Math. Soc.* (*Ser.* 2), **20**, 196–211.

WARHAFT, Z. & LUMLEY, J. L. 1978 An experimental study of the decay of temperature fluctuations in grid-generated turbulence. *J. Fluid Mech.* **88**, 659–684.

WILSON, D. J., ROBINS, A. G. & FACKRELL, J. E. 1982 Predicting the spatial distribution of concentration fluctuations from a ground level source. *Atmos. Env.* **16**, 497–504.

WILSON, D. J., FACKRELL, J. E. & ROBINS, A. G. 1982 Concentration fluctuations in an elevated plume: a diffusion–dissipation approximation. *Atmos. Environ.* **16**, 2581–2589.